Original Article

Biofpr Biofuels Bioproducts & Biorefining

Malic acid production by *Aspergillus oryzae*: the immobilized fungal fermentation route

Hendrik G. Brink, Monique Geyer-Johnson, Reuben M. Swart, Willie Nicol, Department of Chemical Engineering, University of Pretoria, Pretoria, South Africa

Received February 02 2022; Revised September 09 2022; Accepted September 15 2022; View online October 18, 2022 at Wiley Online Library (wileyonlinelibrary.com); DOI: 10.1002/bbb.2440; *Biofuels, Bioprod. Bioref*. 17:363–379 (2023)

Abstract: It has been proposed that the microbial bioproduction of chemical precursors could reduce societal overreliance on the petrochemical industry. However, economic implementation remains elusive due to a lack of understanding of the mechanisms involved. The current study evaluated malic acid production using a novel immobilized *Aspergillus oryzae* fungal bed bioreactor. The experimental procedures involved two different nitrogen sources (urea and $(NH_4)_2SO_4$), two-phase growth/production and simultaneous single-step growth/production runs, the presence and absence of added CO_2, the presence and absence of pH control, and the use of glucose and DL-malate as the carbon sources. The experimental malic acid titers were remarkably poor (between 1.7 and 3.3 $g.L^{-1}$) in comparison with $CaCO_3$ buffered malic acid titers from literature (concentrations in excess of 100 $g.L^{-1}$ have been reported reported). In contrast, citric acid was observed to be the main metabolite. The DL-malate carbon source was consumed with concomitant growth, indicating *A. oryzae*'s ability to utilize both D and L enantiomers of malic acid. Detailed metabolic flux analyses predicted partial consumption of urea during growth, while $(NH_4)_2SO_4$ was fully utilized. During the urea runs, significant amounts of glycogen were accumulated in the biomass – which were utilized as substrate during the production run. Nitrogen limitations induced significant lipid production, corresponding to citric acid accumulation in the media; the mechanism for fungal lipid biosynthesis involves citric acid excretion at the expense of malic acid. These results indicate a possible calcareous trigger for malic acid production as opposed to the traditionally accepted nitrogen starvation mechanism – nitrogen starvation resulted in lipid accumulation with corresponding malate loss. © 2022 The Authors. *Biofuels, Bioproducts and Biorefining* published by Society of Industrial Chemistry and John Wiley & Sons Ltd.

Key words: *Aspergillus oryzae*; malic acid; immobilized biomass fermentation

Introduction

The development of a sustainable society requires a significant industrial shift away from petroleum-based products and towards renewable and bio-based technologies. This shift has been supported by renewed interest by consumers in natural, biodegradable, and environmentally friendly products.[1] As part of its drive towards bio-based products, the US Department of Energy has identified 12 priority platform chemicals required for

Correspondence to: Hendrik G. Brink, Department of Chemical Engineering, University of Pretoria, Lynnwood Road, Pretoria, South Africa. E-mail: deon.brink@up.ac.za

bio-based chemical production; the four carbon dicarboxylic acids, malic-, succinic-, and fumaric acids, being part of this list.[2] The current worldwide demand for malate is reported to be 200 kt per annum[3] whereas the current international supply of L-malic acid is estimated at 40 kt per annum.[4] Malic acid is currently produced commercially by the catalytic hydration of maleic or fumaric acid, which are both derived from maleic anhydride. Maleic anhydride is, in turn, produced from vapor phase oxidation of hydrocarbons, most prominently butane.[5] Unfortunately, this synthetic pathway produces a racemic mixture of L- and D-malic acid, which is unsuitable for the food and beverage industry where malic acid is utilized as an acidulant.[6]

The biological production of malic acid provides stereo selectivity because L-malic acid is a key intermediate in the tricarboxylic acid cycle (TCA) present in most microorganisms.[7] Filamentous fungi of the genus *Aspergillus* have been shown to be superior producers of various bio-based chemicals including lipases,[8] xylanase,[9] and various organic acids; *Aspergillus flavus* and *A. oryzae* widely considered the best biological producers of malic acid.[10] However, *A. flavus* is known to produce hazardous amounts of carcinogenic aflatoxin, making the malic acid produced unsuitable for the food industry. In contrast, *A. oryzae* is a 'generally regarded as safe' (GRAS) organism that does not produce mycotoxins and has therefore been used in the production of sake, shochu, soy sauce, and miso for centuries.[11]

Malic acid cultivation traditionally occurs in a two-step system consisting of a seed culture and an acid production culture under aerobic conditions with a high glucose concentration, a nitrogen source, inorganic salts, and a neutralizing agent. This two-step process facilitates the required high nitrogen concentrations during initial biomass cultivation followed by nitrogen starvation conditions required for malate synthesis.[12] Currently, these laboratory-scale methods have limitations due to the use of pellet morphology and $CaCO_3$ as the go-to buffering agent, which complicates downstream processing.[13] The malic acid metabolism of *A. oryzae* has also not been comprehensively studied specifically with regards to the trigger of malic acid and maximizing this response without the need for metabolic engineering.[14]

The current investigation aimed to develop and test a high density attached biomass reactor with pH control using NaOH. The reactor had the capability to grow biomass aseptically and theoretically produce malic acid in a two-step (growth and production) or one-step combined growth/production process. The study also tested the ability of the organism to reassimilate added malate extracellularly as this would provide insights into the organism's motivation for malate production. Finally, the observed results were analyzed extensively using metabolic flux analyses in an attempt to elucidate the observed results, thereby providing much needed insights into the fungal physiology.

Materials and methods

Microorganism and inoculum preparation

The studied microorganism was wild-type *A. Oryzae* (NRRL 3488, ATCC 56747, or DSM 1863) from the Agricultural Research Service Culture Collection in Peoria, IL, USA. The stock cultures were stored at −40 °C in a 50% $w.w^{-1}$ glycerol solution. Potato dextrose agar (PDA) (Merck KgaA, Darmstadt, Germany) plates were inoculated with the stock solution and incubated at 30 °C for 7 days. Approximately 60 mg of spores (*circa* 6.7×10^8 spores[15]) were harvested from two agar plates with sterilized distilled water. The inoculum was prepared by adding the spore solution to a 10% $w.w^{-1}$ glycerol solution, which was subsequently stored at −40 °C.

Growth and production media

Three different growth media were tested for initial *A. oryzae* growth (GP1, GP2, GP3), varying only in the initial amount of urea ($(NH_2)_2CO$) added to the respective media (2, 0.5 and 0.3 $g.L^{-1}$). The composition of the growth media was based on that of Shigeo *et al.*,[16] Battat *et al.*,[17] and Brown *et al.*,[18] and consisted of a carbon source, a nitrogen source, water, salts, and micronutrients. The growth medium subsumed of (in $g.L^{-1}$): 40 glucose, 0.75 KH_2PO_4, 0.75 K_2HPO_4, 0.1 $MgSO_4 \cdot 7H_2O$, 0.005 $FeSO_4 \cdot 7H_2O$, 0.1 $CaCl_2 \cdot 2H_2O$, and 0.005 NaCl. The production medium (GP3 only) consisted of (in $g.L^{-1}$): 100 glucose, 0.1 KH_2PO_4, 0.1 K_2HPO_4, 0.1 $MgSO_4 \cdot H_2O$, 0.005 $FeSO_4 \cdot 7H_2O$, 0.1 $CaCl_2 \cdot 2H_2O$, and 0.005 NaCl.

For both one-step fermentation experiments (GP4/PP4, GP5/PP5), a medium adapted from Shigeo *et al*[16] was used, which consisted of (in $g.L^{-1}$): 60 glucose, 0.2 $(NH_4)_2SO_4$, 0.75 KH_2PO_4, 0.75 K_2HPO_4, 0.1 $MgSO_4 \cdot 7H_2O$, 0.1 $CaCl_2 \cdot 2H_2O$, 0.005 $FeSO_4 \cdot 7H_2O$, and 0.005 NaCl.

For the malate carbon source experiment (MG) the growth medium contained (in $g.L^{-1}$): 10 DL-malic acid; 0.5 $(NH_4)_2SO_4$; 0.15 KH_2PO_4; 0.15 K_2HPO_4; 0.1 $MgSO_4 \cdot H_2O$; 0.0005 $FeSO_4 \cdot 7H_2O$; 0.1 $CaCl_2 \cdot 2H_2O$ and 0.005 NaCl.

All chemicals were obtained from Merck KgaA (Darmstadt, Germany) unless otherwise specified. The three parts of the nutrient solution (phosphates, sulfates, and chlorides), glucose and nitrogen source were all autoclaved separately at 121 °C for 60 min and mixed aseptically once cooled to room temperature. This was a precautionary measure in the

event that a salt underwent exothermic dissolution, which could have resulted in irreversible ionic precipitation altering the pH and removing valuable compounds that the micro-organism required.

Reactor design

An upscaled version of the novel reactor designed by Naude & Nicol,[19] as seen in Fig. 1, was used. The main components were constructed from aluminium due to its ability to withstand the high pressure and temperature experienced during the sterilization process without deforming or cracking.

A 70 mm outer diameter (OD) × 5 mm wall thickness × 500 mm long glass cylinder was housed between the base and head of the reactor. The reactor had a working volume of 1.1 L. A 34 mm OD × 390 mm polypropylene (PP) pipe, roughened both inside and outside, was used as the immobilization surface for the fungi. Silicone tubing (5 and 10 mm) and PP T-pieces were used to connect the various components in the system. Gas inlets, outlets, and reservoir (product, outlet, etc.) vents had 0.2 μm polytetrafluoroethylene (PTFE) membrane filters attached to them to prevent contamination in the system. The inlet gas consisted of a mixture of 22% O_2 and 78% N_2 (Afrox, Johannesburg, South Africa) and was controlled at specific flowrates using a SLA5850 Brooks mass flow controller (Brooks Instrument, Hatfield, PA, USA). The temperature and pH were measured in the recycle line using a CPS71D digital glass probe. This was connected to a Liquiline CM442 transmitter, which controlled the NaOH dosing pump and the temperature. The dissolved oxygen (DO) was measured using the COS22D dissolved oxygen probe connected to the Liquiline transmitter. The reactor temperature was maintained at 34 °C using the hotplate (Heidolph MR HEI-standard, Heidolph Instruments, Schwabach, Germany) and a custom-designed Proportional-Integral-Derivative (PID) controller integrated within the Labview program.[19] The pH for the glucose-fed runs were controlled at a pH of 6 using 10 mol.L^{-1} NaOH dosed using a peristaltic pump linked to a relay switch; no active pH control was implemented for the malate-fed run. Watson Marlow 120 U peristaltic pumps (Watson Marlow, Falmouth, UK) were used for the inlet, outlet, and dosing pumps. The entire reactor consisted of autoclavable materials.

The CO_2 and O_2 compositions (%) of the outlet air was measured with a tandem gas analyzer (Magellan Instruments Ltd, Middlesex, UK) where the percentage reported indicated the mole percent of the CO_2 and O_2 gas in the gas stream. The CO_2 was measured with infrared red absorption and the O_2 with electrochemical galvanic action which ensured that the sensor output was unaffected by cross-interference from other gases. The gas was also dried through a 0.2 μm PTFE filter (Midisart 2000, Sartorius, Goettingen, Germany) to ensure excess water and ethanol vapor was removed before entering the gas analyzer. These measurements were recorded online using a custom developed LabView (National Instruments, Austin, TX, USA) program. Samples were withdrawn from the reactor using the outlet pump with the first 5 mL discarded to account for the liquid that remained in the tubes from the previous sampling.

Experimental runs

The details of the six different experimental runs are summarized in Table 1. All experiments were initiated by autoclaving the entire reactor system at 121 °C to ensure sterility. The reactor was filled and drained twice using the appropriate growth medium, to remove any remaining water from cleaning and/or autoclaving the reactor. Prior to inoculation, the gas lines were connected and the reactor was allowed to reach a steady state i.e. constant process conditions (%O_2, %CO_2, pH, temperature, DO). The reactor was subsequently inoculated with a thawed (in ice water for 4 h) glycerol inoculum (described above) yielding an initial spore concentration of approximately 54 mg.L^{-1} spores (6.1×10^5 spores.mL^{-1}).

For production phase (PP) the growth medium from GP3 was drained and the reactor filled and drained twice with the PP3 production medium to ensure that any excess nitrogen was washed out prior to production.

The one-step runs (GP4/PP4, GP5/PP5, and MG) were maintained for the full duration of the experiments with no removal or addition of media during the experimental runs.

Based on the size of the reactors it was assumed that any dilutionary effects due to the pH control in runs PP3, GP4/PP4, GP5/PP5 were negligible – this was validated at the end of each run. It was found that there was insufficient acid production in any of the runs for the NaOH addition to make a significant contribution the dilution in the reactor.

Analytical methods

The concentrations of glucose, glycerol, ethanol, and organic acids in the samples were determined with Agilent 1260 Infinity high-performance liquid chromatography (HPLC) equipment (Agilent Technologies, Santa Clara, CA, USA) fitted with a refractive index detector. Samples (± 1 mL) were centrifuged at 16 600×*g* for 90 s and filtered with 0.45 μm Nylon (Minisart) syringe filters into HPLC

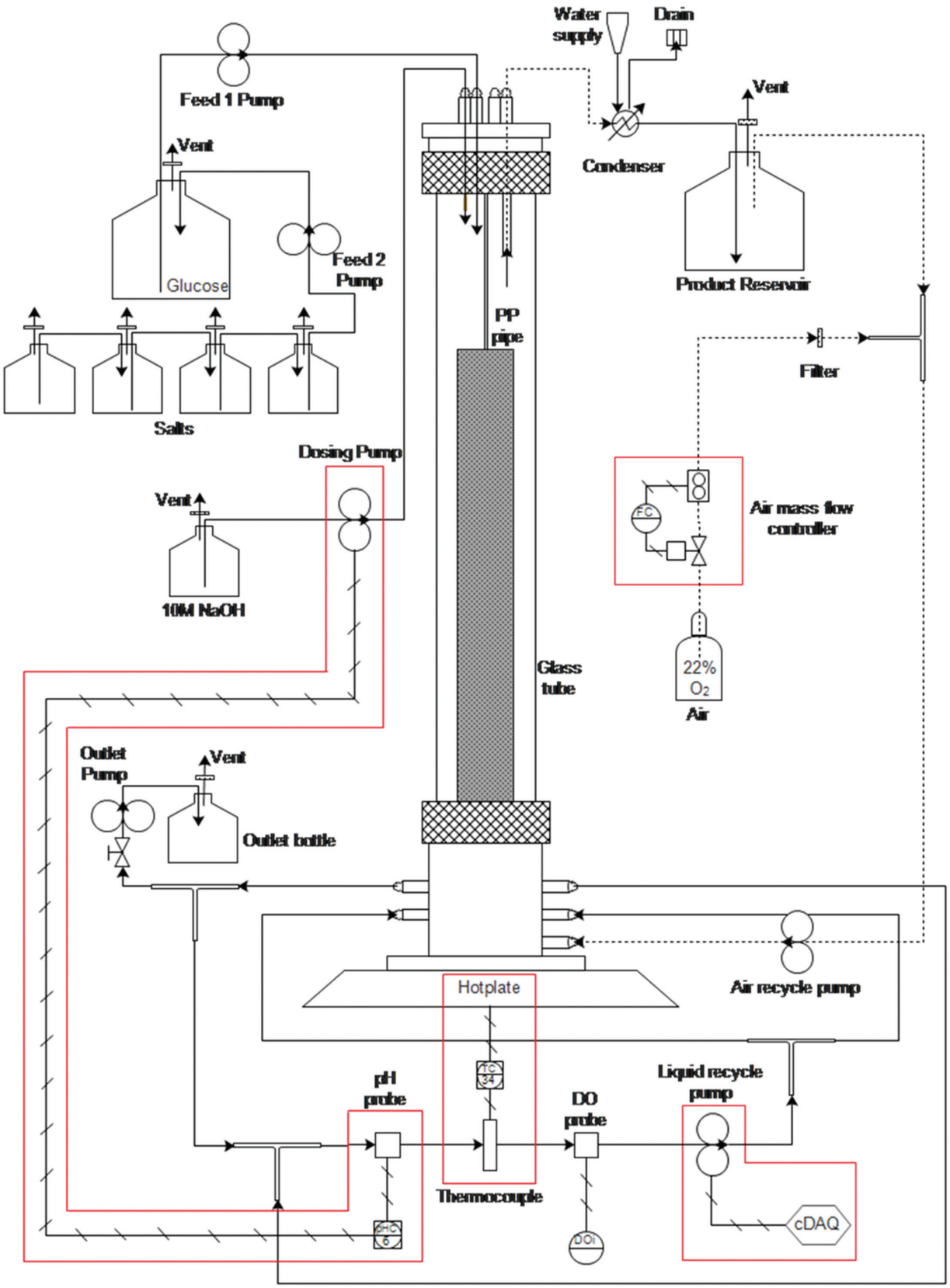

Figure 1. Schematic of the assembled bioreactor system where red blocks indicated the control loops, and the dotted lines were the gas lines.

Table 1. The experimental conditions tested.

Experiment*	Nitrogen source	Nitrogen source Concentration ($g.L^{-1}$)	Carbon source	Carbon source Concentration ($g.L^{-1}$)	CO_2 supply (% in gas feed)	pH control**
GP1	Urea	2	Glucose	40	0	–
GP2	Urea	0.5	Glucose	40	0	–
GP3	Urea	0.3	Glucose	40	0	+
PP3	–	–	Glucose	100	0	+
GP4/PP4	$(NH_4)_2SO_4$	0.2	Glucose	100	0	+
GP5/PP5	$(NH_4)_2SO_4$	0.2	Glucose	100	5	+
MG	$(NH_4)_2SO_4$	0.5	DL-malate	10	0	–

*GP: growth phase. PP: production phase. MG: malic growth.
**– No pH control. + With pH control.

vials and loaded into the autosampler tray of the HPLC equipment. Samples (5 µL) were injected on a Micro-Guard cartridge (30 m × 4.6 m) that was attached to a 300 mm × 7.8 mm Aminex HPX-87H ion-exchange column (Bio-Rad Laboratories, Hercules, CA, USA) maintained at 60 °C. Organic acids and glycerol were measured with mobile phase A (0.02 M H_2SO_4) and glucose, lactic acid, and ethanol with mobile phase C (0.002 M H_2SO_4) both at a flow rate of 0.6 $mL.min^{-1}$. The biomass grown during the growth runs (GP1 and GP2) was removed from the PP pipe and the fermentation medium was filtered through pre-weighed filter paper (47 mm Whatman, Sigma Aldrich, Johannesburg, South Africa). The biomass was washed twice with distilled water to remove any excess dissolved glucose present and dried in the oven at 90 °C for at least 24 h after which it was weighed for final quantification of biomass grown during the run.

Results

Urea growth experiments

During GP1 and GP2, a uniform layer of fungal biomass was observed (Fig. 2), this indicated that the immobilization strategy was successful with negligible planktonic biomass observed in the recycle medium.

The results from the growth runs (GP1 and GP2) are shown in Fig. 3 and clearly demonstrate active respiration (O_2 consumption and CO_2) present during growth. The minor production of metabolites was further observed, with the main metabolites malic acid (MA) and pyruvic acid (PA), with ethanol (ETH) being produced after 15 h, in the GP1 run. Malic acid and citric acid (CA) were the most prominent metabolites observed in GP2.

Figure 3(a) also shows the depletion of dissolved oxygen in the liquid medium, which demonstrates an oxygen mass

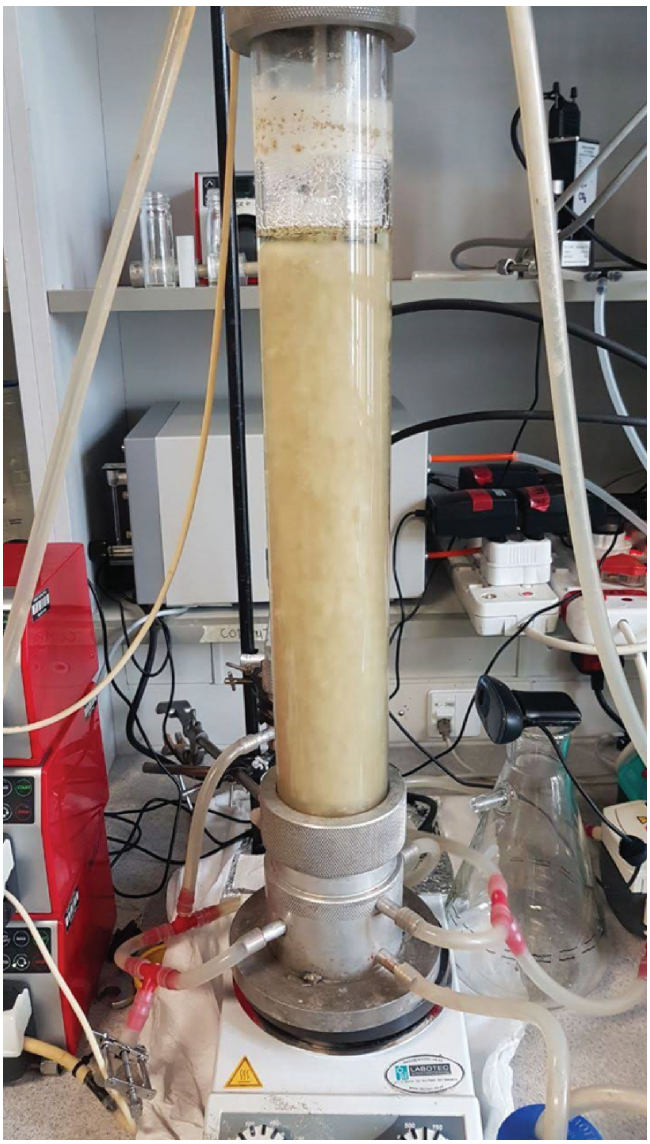

Figure 2. Photograph of immobilized reactor after completion of growth phase.

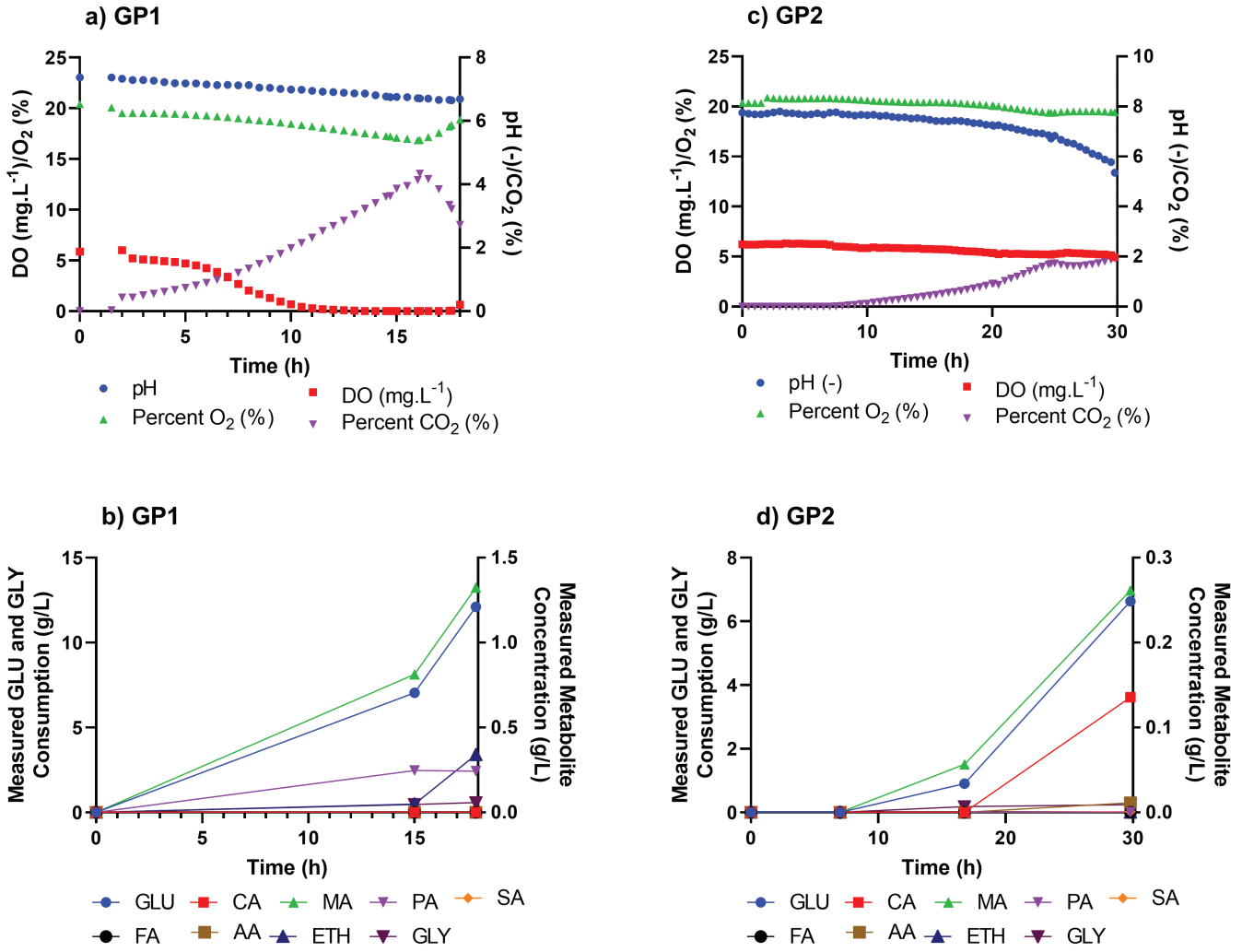

Figure 3. The inline measured variables (a and c) and the HPLC-measured variables (b and d) for GP1 and GP2, respectively. The substrates measured were glucose (GLU) and glycerol (GLY) – The GLY were introduced during inoculation of the reactor. The metabolites measured were citric acid (CA), malic acid (MA), pyruvic acid (PA), succinic acid (SA), fumaric acid (FA), acetic acid (AA) and ethanol (ETH).

transfer limitation, i.e. the rate of oxygen consumption was limited by the diffusion of oxygen into the reaction system. It is known that the gas–liquid mass transfer rate can be expressed by Eqn (1)[20,21]:

$$GTR = k_L a\left(G^* - G\right) \quad (1)$$

in which GTR is the gas transfer rate (mg.(L.h)$^{-1}$), $k_L a$ the gas liquid mass transfer coefficient (h^{-1}), G^* the saturation concentration of the gas at the gas-medium interface (mg.L^{-1}) and G the concentration of the gas in the liquid phase (mg.L^{-1}). Note that the G^* is not the maximum solubility of gas in the liquid phase, but rather G^* is proportional to the partial pressure of the gas in the vapor phase (as per Henry's law) due to the gas–liquid equilibrium at the gas liquid interface.[20,21] The limitation on oxygen transfer is possibly a reason for the production of ethanol after 15 h in GP1 – ethanol yields ATP, supplementing energy under oxygen stressed conditions.[22]

It can further be seen that, except for the initial lag phase, there was a constant flow of CO_2 measured out of the reactor (the reactor headspace was continuously displaced). This means that there was a transfer of CO_2 from the liquid phase to the gas phase (a negative transfer rate according to Eqn 1) due to a greater CO_2 concentration in the liquid phase than the gas liquid interface resulting from a net production of CO_2.

GP1 and GP2 were prematurely terminated at 18 h and 30 h, respectively, due to the observation of excessive

growth, which made transitioning to the production phase infeasible. The fungal biomass for both GP1 and GP2 was removed from the reactor, dried, and weighed. The dry weights measured were 8.73 and 5.19 $g.L^{-1}$, respectively. GP3 subsequently operated at a decreased urea concentration of 0.3 $g.L^{-1}$.

Two-step fermentation process

The results from GP3 and PP3 are shown in Fig. 4. As seen in Fig. 4(a) the $\%O_2$ in the gas outlet as well as DO content decreased throughout GP3, while the $\%CO_2$ still increased. This is consistent with the expected consumption of oxygen coupled with the production of CO_2 due to respiration satisfying the fungal ATP requirements during growth. It can further be observed that the first dosing of 10 M NaOH occurred around 28 h thereby maintaining the pH above 6 as desired. Approximately 5.5 $g.L^{-1}$ of the glucose was consumed during GP3 (Fig. 4b) demonstrating that glucose was at all times in excess. After 32 h there was approximately 0.47 $g.L^{-1}$ MA and 0.13 $g.L^{-1}$ PA measured. Consequently, it was assumed that MA production had been initiated and therefore the reactor content was replaced with the production medium as described above.

The production phase for this experiment lasted 205 h and the inline and HPLC profiles can be seen in Fig. 4(c,d), respectively. The initial $\%CO_2$ dropped to approximately 0.7% after 70 h, after which it remained relatively constant for the duration of the fermentation; this change might indicate a change in the metabolism of the fungi as the ratio of CO_2 to O_2 of an organism provides an indication of activity of the metabolic pathways.[23] It is interesting to note that the production of ETH initiated at the start of PP3; however, at approximately 70 h (the same point where the $\%CO_2$ reached a new constant value) the ETH concentration started decreasing. It can further be observed that a nearly constant percentage of O_2 as well as DO was measured in the reactor. The sufficiently high DO values indicated that the system was not constrained by oxygen mass transfer limitations –the observed ETH production in the first 70 h is therefore unlikely to be a result of anaerobic fermentation conditions and likely indicates Crabtree positive behavior due to glucose overflow in the metabolism.[24] This would need to be verified. The CO_2 percentage values PP3 showed that a net production of CO_2 was present in the reaction system at all times – implying that CO_2 limitations required for anaplerotic reactions are unlikely to be the reason for the limited metabolite production observed during PP3. The MA production rate was higher during the first 70–100 h (2.79 $g.L^{-1}$ malic acid produced) after which production plateaus only increased another 0.5 $g.L^{-1}$ in the remaining 100 h. Only 7.5 $g.L^{-1}$ of glucose was consumed after 205 h, which was ~6% of the initial glucose supplied. This was significantly lower than the glucose consumption rates seen in the literature (using $CaCO_3$ as buffer) where Ochsenreither *et al.*[10] consumed ~80 $g.L^{-1}$ after 220 h, Knuf *et al.*[12] consumed ~35 $g.L^{-1}$ after 48 h and 65.4 $g.L^{-1}$ consumption after 168 h seen by Ding *et al.*[25] Citric acid became the main catabolite after 65 h with 5.98 $g.L^{-1}$ measured at the end of fermentation, followed by malic acid and then acetic acid. The main by-products reported in the literature were succinic acid and fumaric acid, which were measured in small amounts in the current study (0.54 and 0 $g.L^{-1}$, respectively). The amount of malic acid produced (3.34 $g.L^{-1}$) was low for the cultivation period because this was tenfold less than that achieved by Ochsenreither *et al.*[10] where ~40 $g.L^{-1}$ of malic acid was produced over the same period and approximately 40 times slower than Knuf *et al.*[12] that produced the same amount as this study after 5 h of cultivation. These are not the only examples where the malic acid production rate is significantly higher than those in the current study with most of the literature (using $CaCO_3$ as buffer) obtaining higher production rates and titers for malic acid production with *A. oryzae*. Kövilein *et al.*[26] provide a good comparison between *A. oryzae* fermentations using suspended and immobilized biomass and $CaCO_3$ as neutralizing agent. Kövilein *et al.*[26] found that a negligible effect of immobilization on MA production was observed. Even though the immobilization procedure is considerably different in the reference study as compared to the current study (mycelium is suspended in agar vs. mycelium attached to a polypropylene tube), the effect on the mycelium is likely similar. This suggests that the greatest influence on the acid distribution is in fact the neutralizing agent ($CaCO_3$ vs NaOH).

One-step fermentation process

The results from the two one-step fermentation experiments (GP4/PP4 and GP5/PP5) can be seen in Fig. 5. Based on the changes in measured CO_2 and O_2, the exponential growth phase ceased after 24 h and 12 h for the GP4 and GP5 runs, respectively. After these points the system apparently changed metabolic profiles – as evidenced by the marked changes in O_2 and CO_2 percentages in the outlet.

After approximately 40 h, only circa 10% of the initial glucose was consumed in both experiments, with ETH in the case of GP4/PP4 (0.5 $g.L^{-1}$), CA (0.5 and 1.36 $g.L^{-1}$, for GP4/PP4 and GP5/PP5, respectively), and CO_2 the main catabolites. Even though the growth phase ended significantly

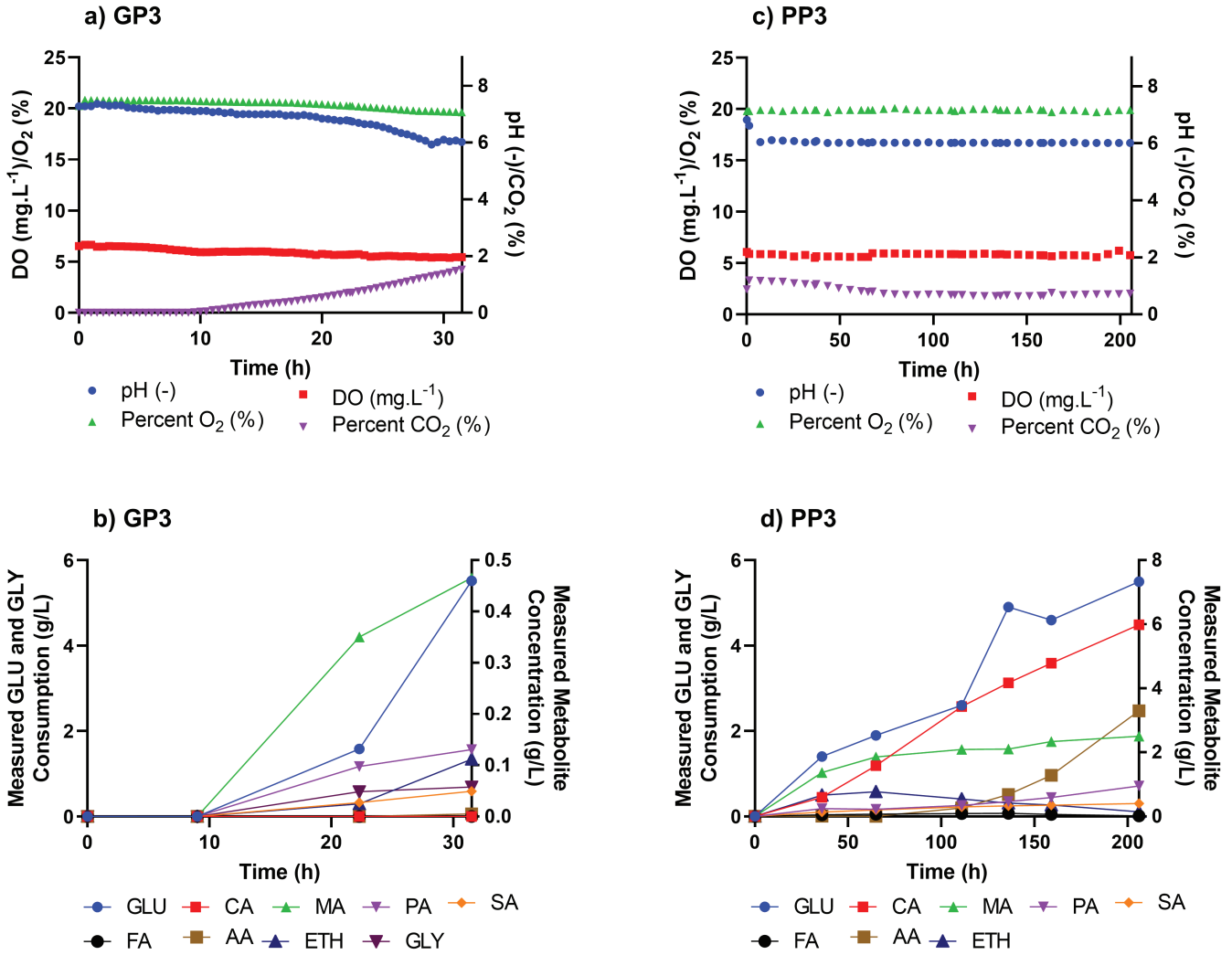

Figure 4. The inline measured variables (a and c) and the HPLC measured variables (b and d) for GP3 and PP3, respectively. The substrates measured were glucose (GLU) and glycerol (GLY) – The GLY were introduced during inoculation of the reactor. The metabolites measured were citric acid (CA), malic acid (MA), pyruvic acid (PA), succinic acid (SA), fumaric acid (FA), acetic acid (AA) and ethanol (ETH).

before the 40 h mark, suggesting nitrogen starvation, there was no malic acid measured in the fermentation broth for either of the experimental runs (Fig. 5b,d).

In the case of run without CO_2 supplementation (GP4/PP4), the MA started increasing after approximately 40 h; however, only a final MA titer of 1.3 $g.L^{-1}$ was measured at the termination of the experiment after 93 h. In contrast, the CO_2 supplemented run (GP5/PP5) showed no MA produced up to the 112 h point while a small amount of pyruvic acid measured (0.29 $g.L^{-1}$). These results strongly indicate that CO_2 limitations do not contribute to the significantly lower MA titers and rates in the current study, in comparison with those observed in literature using $CaCO_3$ as buffer agent in shake flasks.[6,10,12,14]

Growth of *A. oryzae* with malic acid as carbon source

The feasibility of *A. oryzae* NRRL 3488 consuming malic acid as its sole carbon source for growth was tested in the immobilized bio-reactor (MG). The ability to consume organic acids for metabolic activities would give *A. oryzae* a competitive advantage in its natural habitat. The pH and DO were measured as previously described, with no active pH control employed.

The consumption of DL-malic acid can be seen in Fig. 6(a) where most of the DL-malic acid was consumed after 260 h. This showed that *A. oryzae* NRRL 3488 could consume both isomers of malic acid and not just L-malic

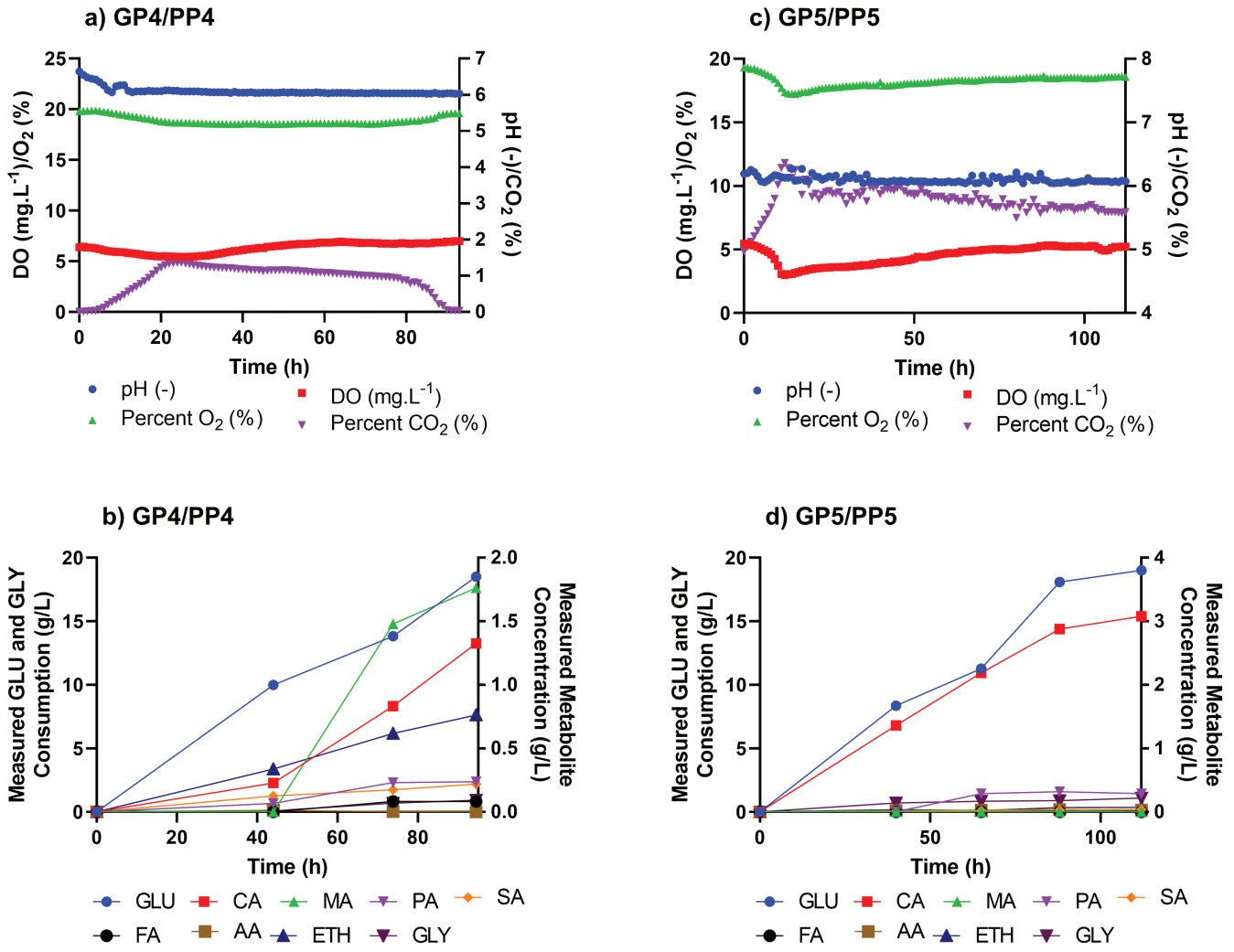

Figure 5. The inline (a and c) and HPLC (b and d) measurements in the one-step fermentation runs GP4/PP4 and GP5/PP5 respectively. The substrates measured were glucose (GLU) and glycerol (GLY) – The GLY were introduced during inoculation of the reactor. The metabolites measured were citric acid (CA), malic acid (MA), pyruvic acid (PA), succinic acid (SA), fumaric acid (FA), acetic acid (AA) and ethanol (ETH).

acid, which was the naturally occurring form. Based on the change in $\%CO_2$ measured, there was an initial growth phase up to 50 h, followed by a stationary phase to around 80 h and then a second exponential growth phase, which ended after 200 h. At the end of cultivation, there was 0.13 $g.L^{-1}$ glycerol, 0.13 $g.L^{-1}$ of fumaric acid and 0.26 $g.L^{-1}$ of ethanol measured. There was minimal change in the $\%O_2$ measured in the gas outlet throughout the cultivation period (Fig. 6b) where the DO concentration increased with the $\%CO_2$.

These results showed that *A. oryzae* NRRL 3488 only required a small amount of O_2 for growth on DL-malic acid and that it could consume both D- and L-malic acid. The pH started increasing around the second exponential growth phase and showed *A. oryzae*'s resilience to not only grow in a low pH but to consume an acidic carbon source to survive. This would give *A. oryzae* NRRL 3488 an advantage in nature because it can outcompete over other micro-organisms by converting available substrates (glucose, sucrose, etc.) to organic acids, which it can then later consume as required.

Discussion

To facilitate more in-depth understanding of the observed results as, presented in Fig. 3–6, a detailed metabolic flux analysis was conducted using the method proposed by Villadsen *et al.*[20] A detailed metabolic map for *A. oryzae*

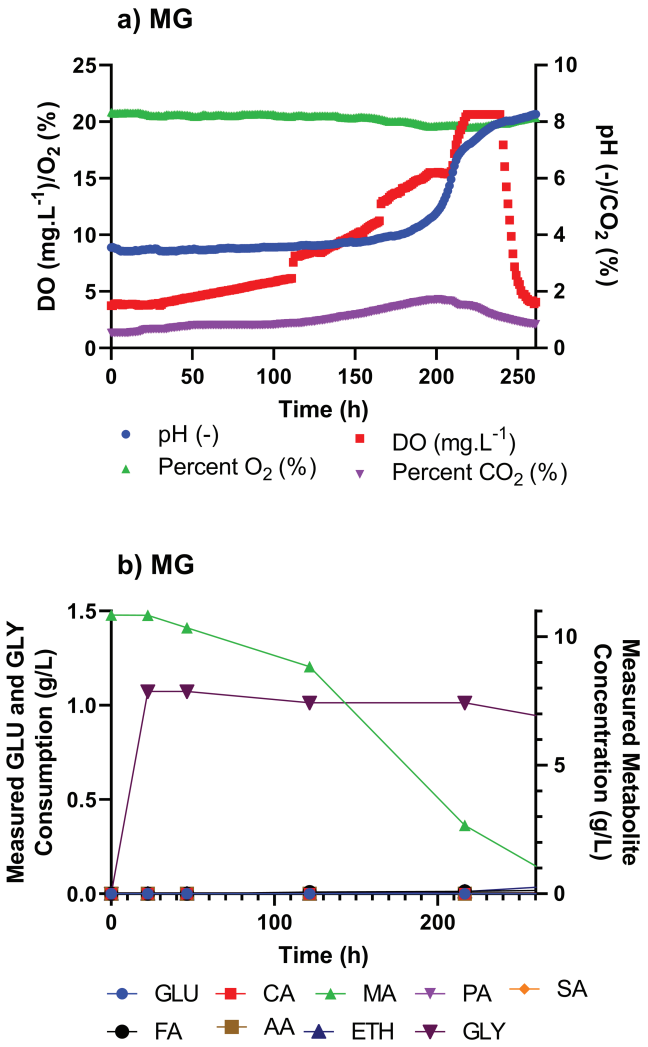

Figure 6. The inline measurements (a) and HPLC measurements (b) for aerobic growth of *A. oryzae* NRRL 3488 with DL-malic acid as the sole carbon source and no pH control. The substrates measured were glucose (GLU) and glycerol (GLY) – The GLY was introduced during inoculation of the reactor. The metabolites measured were citric acid (CA), malic acid (MA), pyruvic acid (PA), succinic acid (SA), fumaric acid (FA), acetic acid (AA), and ethanol (ETH).

NRRL 3488 was obtained from Vongsangnak *et al.*[22] and simplified to produce a metabolic map corresponding to a 20×20 matrix, which could be solved for each time-based set of measurements for the experimental runs (Fig. 7).

The matrix consisted of 20 fluxes (v_i) corresponding to the matrix columns, seven node balances (designated by capital letters) for rows 1–7, NAD(P)H and ATP balances (rows 8–9), and 11 specified rates, i.e. r_{CO_2}, r_{CA}, r_{MA}, r_{PA}, r_{SA}, r_{FA}, r_{AA}, r_{ETH}, r_{GLU}, r_{GLY}, and r_s. The rates were estimated by fitting smooth higher order polynomials to the experimental measurements and finding the first differential at the applicable experimental times.[27]

Due to the significant duplication of the TCA cycle in the mitochondria and the cytosol, as well as the presence of transporters for all TCA intermediate metabolites (except Acetyl-CoA) between the mitochondria and cytosol, no clear distinction could be made between the cytosolic and mitochondrial pathways and therefore the net fluxes were modeled for each TCA pathway – the net being the sum of the cytosolic and mitochondrial pathways (e.g. $v_3 = v_{3,m} + v_{3,c}$). The prevalence of simultaneous NADH- and NADPH-generating enzymes for several mitochondrial and cytosolic pathways, as well as transhydrogenase in the metabolism,[22] necessitated the combination of all redox in the metabolism as NAD(P)H. The values used in the ATP balance ($\gamma = 2.70$ mol ATP.(C-mol biomass)$^{-1}$, $m_{ATP} = 0.015$ mol ATP.(C-mol biomass.h)$^{-1}$ and P/O = 2.17 mol ATP.(0.5 mol O_2)$^{-1}$) were those obtained by Krzystek *et al.* for *Aspergillus niger*.[28] These values were within the order of magnitude of other fungal systems.[29] The biomass was assumed to consist of three main components. First, a proteinaceous active biomass (X) with a formula corresponding to that of standard biomass ($CH_{1.8}O_{0.5}N_{0.2}$).[20] Second, a glycogen (GLN) fraction was assumed in which glucose are stored intracellularly by the fungus – fungi are well known to utilize this mechanism for glucose storage.[30,31] Finally, a lipid fraction (Lip) was assumed – *A. oryzae* is well known as an oleaginous fungus with its lipid production capabilities well documented.[32–37] For the lipid synthesis route, a model lipid (palmitic acid) was used to estimate the NAD(P)H and ATP requirements. It is known that the synthesis of lipids in the metabolism of *A. oryzae* has a common pathway through palmitic acid prior to diversifying into a spectrum of lipids.[22]

The results from the matrix solutions were integrated numerically over the experimental time to yield the accumulated metabolite profiles. The comparisons of the experimentally determined accumulated metabolite concentrations and the predicted concentrations are shown in Fig. 8. The results indicate that the model corresponded exceptionally well to the accumulated metabolite concentration, thereby validating the accuracy of the model in predicting the metabolic behavior of the fungus.

The most significant model results from the model predictions related to the biomass composition as this provided insights into the response of the organism to different operational conditions in the system. Figure 9 shows the cumulative stacked biomass profiles for the experimental runs and show clear differences resulting from the different operational conditions. It should be noted that the biomass

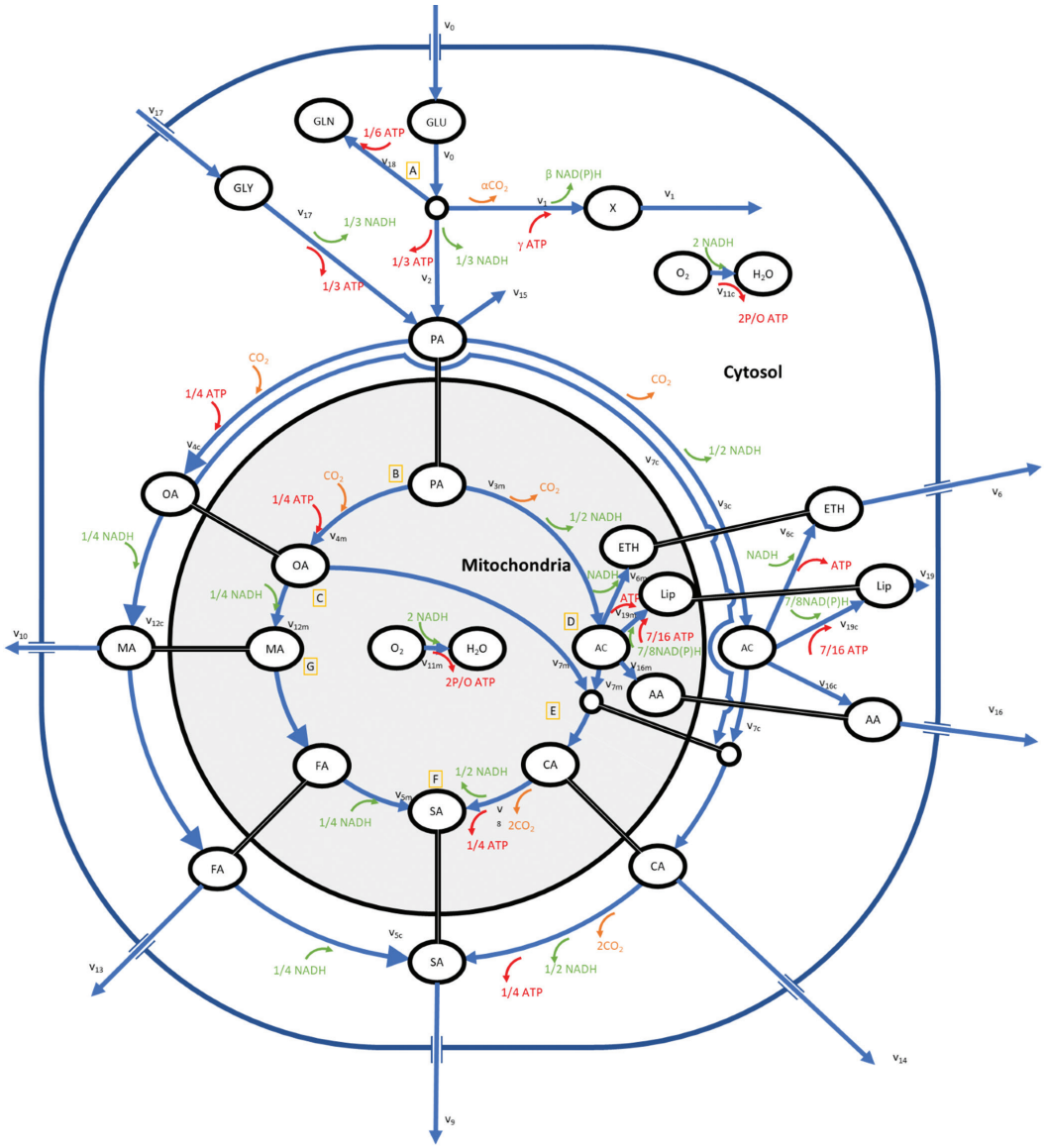

$$
\begin{bmatrix}
 & v_0 & v_1 & v_2 & v_3 & v_4 & v_5 & v_6 & v_7 & v_8 & v_9 & v_{10} & v_{11} & v_{12} & v_{13} & v_{14} & v_{15} & v_{16} & v_{17} & v_{18} & v_{19} \\
A & 1 & -(1+\alpha) & -1 & 0 & 0 & 0 & 0 & 0 & 0 & 0 & 0 & 0 & 0 & 0 & 0 & 0 & 0 & 1 & -1 & 0 \\
B & 0 & 0 & 1 & -\frac{3}{2} & -1 & 0 & 0 & 0 & 0 & 0 & 0 & 0 & 0 & 0 & 0 & -1 & 0 & 0 & 0 & 0 \\
C & 0 & 0 & 0 & 0 & 1 & 0 & 0 & -1 & 0 & 0 & 0 & 0 & -1 & 0 & 0 & 0 & 0 & 0 & 0 & 0 \\
D & 0 & 0 & 0 & 1 & 0 & 0 & -1 & -1 & 0 & 0 & 0 & 0 & 0 & 0 & 0 & 0 & -1 & 0 & 0 & -1 \\
E & 0 & 0 & 0 & 0 & 0 & 0 & 0 & 2 & -\frac{3}{2} & 0 & 0 & 0 & 0 & 0 & -1 & 0 & 0 & 0 & 0 & 0 \\
F & 0 & 0 & 0 & 0 & 0 & -1 & 0 & 0 & -1 & -1 & 0 & 0 & 0 & 0 & 0 & 0 & 0 & 0 & 0 & 0 \\
G & 0 & 0 & 0 & 0 & 0 & 1 & 0 & 0 & 0 & 0 & 1 & 0 & -1 & 1 & 0 & 0 & 0 & 0 & 0 & 0 \\
NAD(P)H & 0 & \beta & \frac{1}{3} & \frac{1}{2} & -\frac{1}{4} & 0 & -1 & 0 & \frac{1}{2} & 0 & 0 & -2 & -\frac{1}{4} & 0 & 0 & 0 & 0 & \frac{1}{3} & 0 & 0.875 \\
ATP & 0 & \gamma & \frac{1}{3} & 0 & \frac{1}{4} & 0 & 1 & 0 & \frac{1}{4} & 0 & 0 & 2P/O & 0 & 0 & 0 & 0 & 0 & \frac{1}{3} & -\frac{1}{6} & -\frac{7}{16} \\
S_1 & 0 & \alpha & 0 & \frac{1}{2} & -\frac{1}{4} & 0 & 0 & 0 & \frac{1}{2} & 0 & 0 & 0 & 0 & 0 & 0 & 0 & 0 & 0 & 0 & 0 \\
S_2 & 0 & 0 & 0 & 0 & 0 & 0 & 0 & 0 & 0 & 0 & 0 & 0 & 0 & 0 & 1 & 0 & 0 & 0 & 0 & 0 \\
S_3 & 0 & 0 & 0 & 0 & 0 & 0 & 0 & 0 & 0 & 0 & 1 & 0 & 0 & 0 & 0 & 0 & 0 & 0 & 0 & 0 \\
S_4 & 0 & 0 & 0 & 0 & 0 & 0 & 0 & 0 & 0 & 0 & 0 & 0 & 0 & 0 & 0 & 1 & 0 & 0 & 0 & 0 \\
S_5 & 0 & 0 & 0 & 0 & 0 & 0 & 0 & 0 & 0 & 1 & 0 & 0 & 0 & 0 & 0 & 0 & 0 & 0 & 0 & 0 \\
S_6 & 0 & 0 & 0 & 0 & 0 & 0 & 0 & 0 & 0 & 0 & 0 & 0 & 0 & 1 & 0 & 0 & 0 & 0 & 0 & 0 \\
S_7 & 0 & 0 & 0 & 0 & 0 & 0 & 0 & 0 & 0 & 0 & 0 & 0 & 0 & 0 & 0 & 0 & 1 & 0 & 0 & 0 \\
S_8 & 0 & 0 & 0 & 0 & 0 & 0 & 0 & 1 & 0 & 0 & 0 & 0 & 0 & 0 & 0 & 0 & 0 & 0 & 0 & 0 \\
S_9 & 1 & 0 & 0 & 0 & 0 & 0 & 0 & 0 & 0 & 0 & 0 & 0 & 0 & 0 & 0 & 0 & 0 & 0 & 0 & 0 \\
S_{10} & 0 & 0 & 0 & 0 & 0 & 0 & 0 & 0 & 0 & 0 & 0 & 0 & 0 & 0 & 0 & 0 & 0 & 1 & 0 & 0 \\
S_{11} & 0 & 0 & 0 & 0 & 0 & 0 & 0 & 0 & 0 & 0 & 0 & 1 & 0 & 0 & 0 & 0 & 0 & 0 & 0 & 0
\end{bmatrix}
\times \overline{p} =
\begin{bmatrix}
0 \\ 0 \\ 0 \\ 0 \\ 0 \\ 0 \\ 0 \\ 0 \\ m_{ATP} \\ r_{CO_2} \\ r_{CA} \\ r_{MA} \\ r_{PA} \\ r_{SA} \\ r_{FA} \\ r_{AA} \\ r_{ETH} \\ r_{GLU} \\ r_{GLY} \\ r_{O_2}
\end{bmatrix}
$$

Figure 7. The simplified metabolism of *A. oryzae* – Adapted from Vongsangnak *et al*.[22] GLU: Glucose. GLN: Glycogen. GLY: Glycerol. X: Active biomass. PA: Pyruvic acid. AC: Acetyl-CoA. ETH: Ethanol. lip: Lipids. AA: Acetic acid. CA: Citric acid. SA: Succinic acid. FA: Fumaric acid. MA: Malic acid. OA: Oxaloacetic acid.

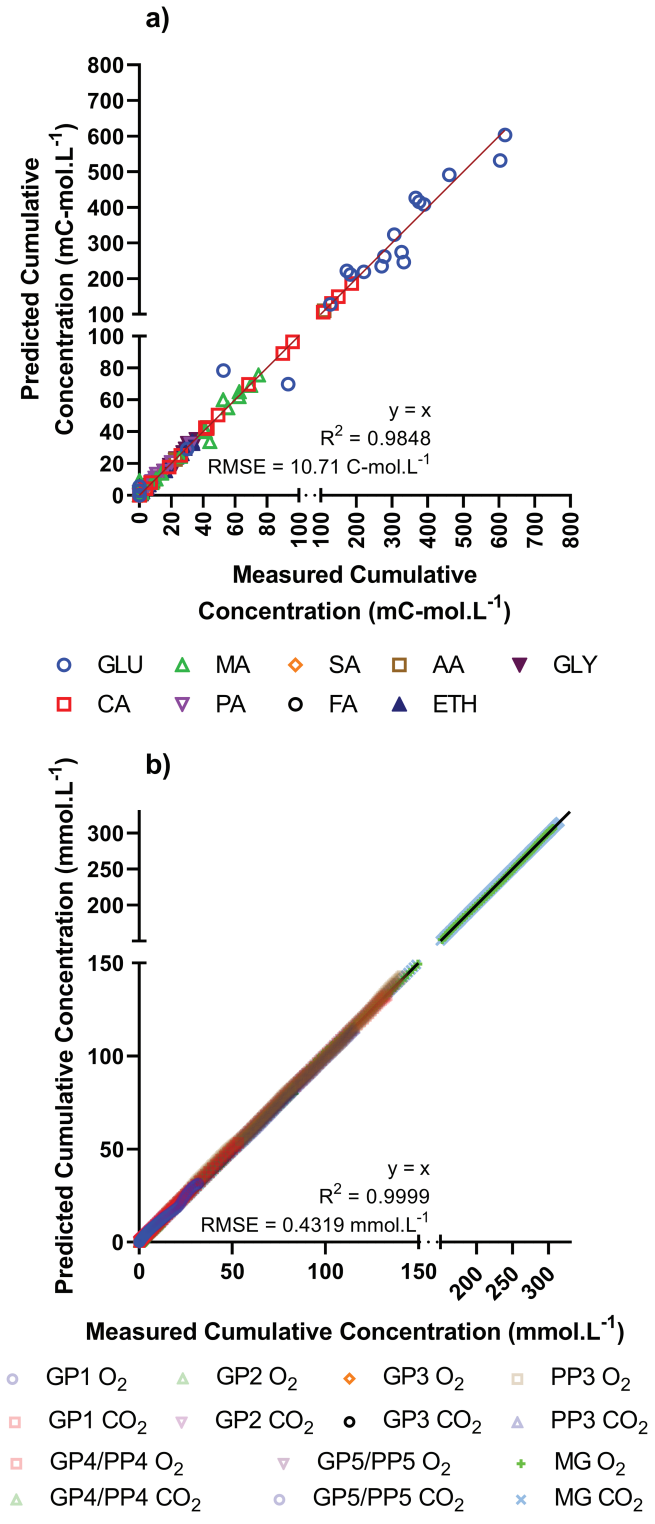

Figure 8. Parity plots of the (a) HPLC measured cumulative metabolite concentrations and (b) O_2 and CO_2 measurements versus the predicted corresponding cumulative values determined from the metabolic flux model.

concentrations for both GP1 (8.83 vs 8.73 g.L^{-1}) and GP2 (5.51 vs 5.19 g.L^{-1}) were within 6% of the measured values determined after their terminations.

When considering Fig. 9, it is clear that the urea runs (GP1, GP2, and GP3) were apparently unable to utilize the urea completely during the growth runs. The biomass was, however, able to grow sufficiently to induce clogging the bioreactor for both GP1 and GP2. The corresponding biomass profiles show that the majority of the biomass in these runs consisted of glycogen – in some case as much as 90% of the biomass. This is however not completely precedented, with 'fattening factors' (ratios of lipids and polysaccharides to active biomass) as high as 10 reported for various fungi in literature.[38] It is of interest that the same profiles were observed for all three urea runs – providing some evidence that these observed trends likely have validity. For PP3, a significant decrease in the GLN was observed indicating that the GLN was consumed as substrate in parallel with the glucose in the medium. This is interesting as there was a significant amount of glucose in the medium (initial concentration of 100 g.L^{-1}), which would imply that the organism should not experience carbon limitations. Upon further investigation, it was observed that the glucose consumption rate during PP3 was only 0.070 ± 0.006 g.(L.h)$^{-1}$, a significant reduction from that for GP3 (0.4214 ± 0.0802 g.(L.h)$^{-1}$), indicating that the access to the vast glucose reserves in the medium was somehow limited. The consumption of GLN in the biomass was also accompanied by Lip synthesis. Interestingly, it has previously been noted that the synthesis of lipids by oleaginous fungi correspond to nitrogen exhaustion (present in PP3, but not GP1, GP2 and GP3) and the concomitant excretion of CA.[39] This can be attributed to the accumulation of CA in the mitochondrion as a result of AMP cleaving by the organism to access NH_4^+ required for maintenance – a process that simultaneously slows the TCA cycle due to a shortage of AMP required for ATP synthesis.[39] The excess CA is eventually transported from the mitochondrion in exchange for cytosolic MA, a CA – MA antiporter is present in *A. oryzae*.[22] In the cytosol, the CA is used as substrate for Lip synthesis with excess CA being transported to the medium.[22] In addition, it is considered that the major supplier of NADPH required for Lip synthesis is supplied by malic enzyme; the enzymatic reaction in which MA is directly converted to PA with an accompanying production of NADPH.[22] These MA restrictive processes, i.e. CA – MA exchange, and the malic enzyme conversion of MA to PA, inherently limits the cytosolic concentration of MA and therefore limits the excretion of MA to the medium. These

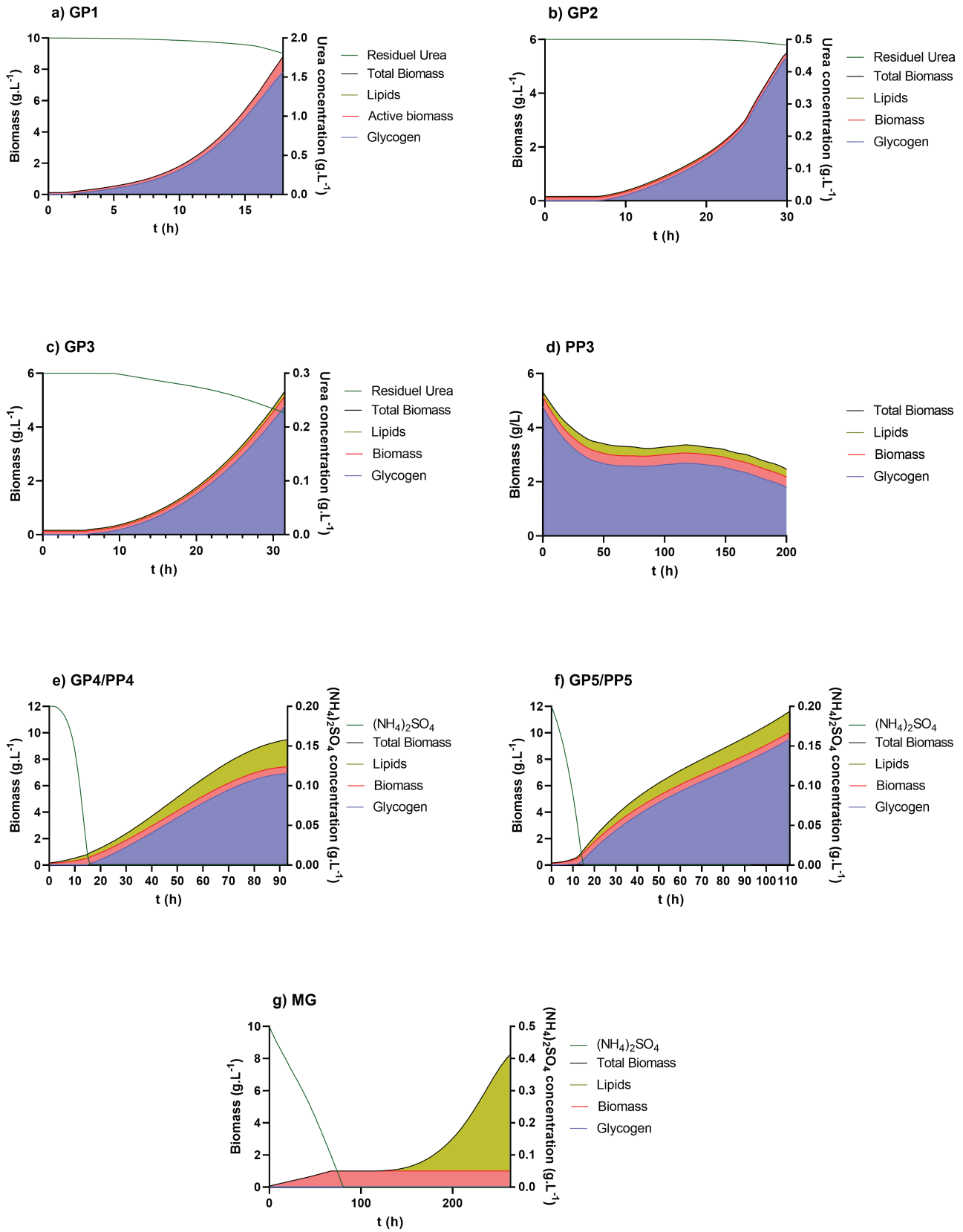

Figure 9. The cumulative stacked biomass composition profiles and the residual nitrogen concentrations for (a) GP1, (b) GP2, (c) GP3, (d) PP3, (e) GP4/PP4, (f) GP5/PP5, (g) MG.

observations correspond well with single-step runs (Fig. 9e) GP4/PP4 and f) GP5/PP5) in which the $(NH_4)_2SO_4$ was utilized rapidly (in comparison with the urea) resulting in nitrogen starvation and corresponding Lip synthesis. These runs also included significant CA accumulation in the medium. Correspondingly, the glucose consumption rates for GP4 and GP5 were markedly greater than that for PP4 and PP5; Fig. 10 shows the glucose (GLU) consumption rates for the experimental conditions as well as a comparison with results from Geyer *et al.*[13]

From Fig. 10(b) it can be seen that there is a positive correlation between the amount of nitrogen fed and glucose consumption rate – a greater amount of nitrogen fed corresponds to a greater glucose consumption rate. It is of interest that the glucose consumption rate at a depleted nitrogen concentration corresponded to approximately 0.11 g.(L.h)$^{-1}$. Further, the nitrogen was not depleted in any of the malic producing runs, supporting the observation that

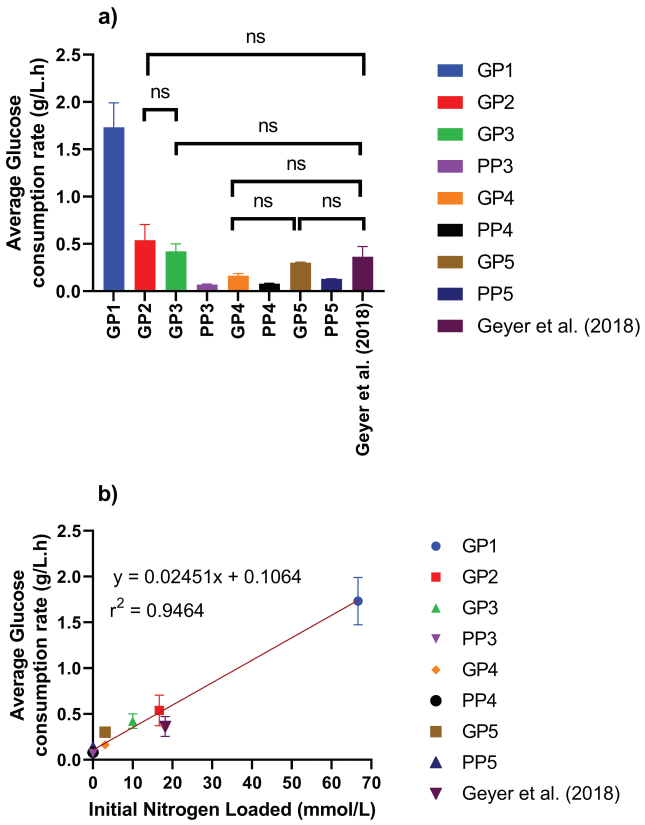

Figure 10. (a) The glucose consumption rates for the experimental runs as well as comparable results from the literature.[13] The brackets indicate insignificant differences at the 5% significance level as calculated using one-way ANOVA analysis. (b) The linear correlation between the initial nitrogen concentration and the average GLU consumption rates.

nitrogen limitation is responsible for CA accumulation as well as limitations in GLU consumption rates. This observation correspond to the results reported by Geyer *et al.,* in which as much as 40 g.L^{-1} of MA was measured in shaker flask runs with approximately 20% (0.24 g.L^{-1} $(NH_4)_2SO_4$) residual nitrogen.[13]

The biomass profile for MA grown *A. oryzae* (Fig. 10g) demonstrate, yet again, the rapid consumption of $(NH_4)_2SO_4$, coupled with the accumulation of Lip. Interestingly, this was not accompanied by the excretion of significant amounts of CA, however considering the nature of the substrate (MA) and the exceptionally slow rate of growth it is likely that the rate-limiting step in the process was the transport and conversion of MA to ATP (in the mitochondrial TCA cycle) while the accumulation of CA in the mitochondria, the transport to the cytosol, and subsequent conversion to Lip were at pseudo equilibrium and therefore no significant accumulation of CA in the cytosol was observed.

The results and analyses propose that nitrogen limitation in the system corresponds to Lip synthesis with limited CA production and a two-pronged destruction of MA, therefore signifying that the system inherently and significantly limits the production of MA. This is in complete contradiction with previously presented work in which it was proposed that nitrogen limitation is the key element required for MA production.[12] From these results it would appear that the main difference between the present study and those from literature is the presence of $CaCO_3$ in the medium. This is consistent with the observations of Geyer *et al.*[13] and Kövilein *et al.*[14] who observed increased production of MA with increased initial concentrations of $CaCO_3$ loaded to the reactors. It has been proposed that fungi and other soil microbes excrete organic acid in calcium-rich soils to liberate nutrients (such as phosphates and metals) precipitated due to the high pH of these soils.[40,41]

In a seminal review paper on the subject of calcium in fungi, Pitt *et al.*[42] provided many insights into the effects of calcium on fungi, some of these included the effects of Ca^{2+} on transport phenomena associated with fungi – e.g. Ca^{2+} is associated with the protection of the fungi from the injurious effect of H^+, K^+ and Na^+ on uptake phenomena, specifically with reference to Na^+. This is of particular interest as the current system pH was controlled by NaOH. In addition, the localization of Ca^{2+} within the fungal physiology (mostly within the mitochondria) and the effects of Ca^{2+} on the morphology of fungi are also known effect of Ca^{2+} in the fungal system. These observation were supported by a more recent review by Lange and Peiter.[43]

in which it was further proposed that many of the effects and interactions of Ca^{2+} with fungal physiology link to the maintenance of Ca^{2+} homeostasis, with multiple channels and transporters dedicated to this task. Consequently, the magnitude of these effects is likely to be complex with synchronous interactions likely – as was observed in a recent study by Ronoh *et al.*[44] in which a compounded interaction between Ca^{2+} and pH were observed to affect the production of MA by *Rhizopus oryzae*.

Conclusions

The main aim of this study was to test the feasibility of using immobilized *A. oryzae* to produce malic acid in a novel bio-reactor with NaOH pH control. This was tested by initially growing an immobilized layer of *A. oryzae* using a growth media with different concentrations of urea to establish the growth characteristics. This was followed by a switch to a nitrogen-starved production medium to induce malic acid production. In addition, this investigation tested a one-step fermentation for simultaneous growth and malic acid production using immobilized *A. oryzae*. These results indicated that a nitrogen-starved environment resulted in significant Lip accumulation due to the deceleration of the TCA cycle, mitrochondrial/cytosolic CA accumulation and consequent Lip synthesis. This process involves the consumption of MA by the exchange of mitochondrial CA for cytosolic MA, and the conversion of MA to PA to produce NADPH, which is required for Lip synthesis. Therefore, these observations directly contradict the proposition that nitrogen limitation is the main requirement for malic acid production. The malic acid production rates and titers obtained with the novel bio-reactor for both the two-step and one-step processes were well below those expected when compared to the literature (utilizing $CaCO_3$ as pH buffer), indicating a potential calcareous requirement for malate production.

Finally, it was also found that *A. oryzae* NRRL 3488 could consume both isomers of malic acid (D and L) for growth at an acidic pH. This observation indicated that extracellular malate can be reassimilated after excretion, providing a survival mechanism that can be utilized by the organism to, first, acidify its environment and, second, convert a sugary substance to a less metabolizable substrate thereby inhibiting competition.

References

1. Mondala AH, Direct fungal fermentation of lignocellulosic biomass into itaconic, fumaric, and malic acids: current and future prospects. *J Ind Microbiol Biotechnol* **42**(4):487–506 (2015).
2. Werpy T and Petersen GR, *Top Value Added Chemicals from Biomass. Volume 1-Results of Screening for Potential Candidates from Sugars and Synthesis Gas*. Golden: National Renewable Energy Laboratory, Golden, CO, USA (2004).
3. Chi Z, Wang ZP, Wang GY, Khan I and Chi ZM, Microbial biosynthesis and secretion of l-malic acid and its applications. *Crit Rev Biotechnol* **36**(1):99–107 (2016).
4. Liu J, Li J, Dong SH, Du G, Chen J and Liu L, Biological production of l-malate: recent advances and future prospects. *World J Microbiol Biotechnol* **34**(1):1–8 (2018). https://doi.org/10.1007/s11274-017-2349-8.
5. Hermann BG and Patel M, Today's and tomorrow's bio-based bulk chemicals from white biotechnology. *Appl Biochem Biotechnol* **136**(3):361–388 (2007 Mar). https://doi.org/10.1007/s12010-007-9031-9.
6. Knuf C, Nookaew I, Remmers I, Khoomrung S, Brown S, Berry A *et al.*, Physiological characterization of the high malic acid-producing *Aspergillus oryzae* strain 2103a-68. *Appl Microbiol Biotechnol* **98**(8):3517–3527 (2014).
7. Liu J, Xie Z, Dong SH, Li J, Du G, Chen J *et al.*, Rewiring the reductive tricarboxylic acid pathway and L-malate transport pathway of *Aspergillus oryzae* for overproduction of L-malate. *J Biotechnol* **253**(May):1–9 (2017). https://doi.org/10.1016/j.jbiotec.2017.05.011.
8. Melo AF, Mauricio EF, Salgado AM, Pellegrini Pessoa FL, Triches Damaso MC and Couri S, Assessment of catalytic properties in aqueous and media of aspergillus Niger lipase immobilized on supports vitreous. *Chem Eng Trans* **24**:973–978 (2011).
9. Park Y, Kang S, Lee J, Hong S and Kim S, Xylanase production in solid state fermentation by aspergillus Niger mutant using statistical experimental designs. *Appl Microbiol Biotechnol* **58**(6):761–766 (2002). http://link.springer.com/10.1007/s00253-002-0965-0.
10. Ochsenreither K, Fischer C, Neumann A and Syldatk C, Process characterization and influence of alternative carbon sources and carbon-to-nitrogen ratio on organic acid production by *Aspergillus oryzae* DSM1863. *Appl Microbiol Biotechnol* **98**(12):5449–5460 (2014).
11. Payne GA, Nierman WC, Wortman JR, Pritchard BL, Brown D, Dean RA *et al.*, Whole genome comparison of *Aspergillus flavus* and *A. oryzae*. *Med Mycol* **44**(Suppl. 1):9–11 (2006).
12. Knuf C, Nookaew I, Brown SH, McCulloch M, Berry A and Nielsen J, Investigation of malic acid production in *Aspergillus oryzae* under nitrogen starvation conditions. *Appl Environ Microbiol* **79**(19):6050–6058 (2013).
13. Geyer M, Onyancha FM, Nicol W and Brink HG, Malic acid production by *Aspergillus oryzae*: the role of CaCO3. *Chem Eng Trans* **70**(July):1801–1806 (2018). www.aidic.it/cet.
14. Kövilein A, Umpfenbach J and Ochsenreither K, Acetate as substrate for l-malic acid production with *Aspergillus oryzae* DSM 1863. *Biotechnol Biofuels* **14**(1):1–15 (2021). https://doi.org/10.1186/s13068-021-01901-5.
15. Smith CS, Slade SJ, Nordheim EV, Cascino JJ, Harris RF and Andrews JH, Sources of variability in the measurement of fungal spore yields. *Appl Environ Microbiol* **54**(6):1430–1435 (1988). https://journals.lww.com/00006396-198805000-00008.
16. Shigeo A, Furuya A, Saito T. Method of producing l-malic acid by fermentation, United States; US3063910A, 1962. p. 3–5.
17. Battat E, Peleg Y, Bercovitz A, Rokem JS and Goldberg I, Optimization of L-malic acid production by aspergillus flavus

in a stirred fermentor. *Biotechnol Bioeng* **37**(11):1108–1116 (1991).
18. Brown SH, Bashkirova L, Berka R, Chandler T, Doty T, McCall K *et al*., Metabolic engineering of *Aspergillus oryzae* NRRL 3488 for increased production of l-malic acid. *Appl Microbiol Biotechnol* **97**(20):8903–8912 (2013).
19. Naude A and Nicol W, Improved continuous fumaric acid production with immobilised *Rhizopus oryzae* by implementation of a revised nitrogen control strategy. *New Biotechnol* **44**(July 2017):13–22 (2018). https://doi.org/10.1016/j.nbt.2018.02.012.
20. Villadsen J, Nielsen J, Lidén G, Bioreaction Engineering Principles [Online]. 3rd ed., New York: Springer (2011). Available: http://books.google.com/books?hl=en&lr=&id=htUeM34b7KgC&oi=fnd&pg=PR8&dq=Bioreaction+engineering+principles&ots=OYAiewkiRp&sig=_OrIEeYgQxEbBKI4QoCfFT-OEzQ [30 January 2012].
21. Scott FH, *Elements of Chemical Reaction Engineering*, 4th edn. Pearson Education Limited, London (2013).
22. Vongsangnak W, Olsen P, Hansen K, Krogsgaard S and Nielsen J, Improved annotation through genome-scale metabolic modeling of *Aspergillus oryzae*. *BMC Genomics* **9**:245 (2008).
23. de Jongh NW, Swart RM and Nicol W, Fed-batch growth of *Rhizopus oryzae*: eliminating ethanol formation by controlling glucose addition. *Biochem Eng J* **169**(November 2020):107961 (2021).
24. Swart RM, Le Roux F, Naude A, De Jongh NW and Nicol W, Fumarate production with *Rhizopus oryzae*: Utilising the Crabtree effect to minimise ethanol by-product formation. *Biotechnol Biofuels* **13**(1):1–11 (2020). https://doi.org/10.1186/s13068-020-1664-8.
25. Ding Q, Luo Q, Zhou J, Chen X and Liu L, Enhancing l-malate production of *Aspergillus oryzae* FMME218-37 by improving inorganic nitrogen utilization. *Appl Microbiol Biotechnol* **102**(20):8739–8751 (2018).
26. Kövilein A, Aschmann V, Hohmann S and Ochsenreither K, Immobilization of *Aspergillus oryzae* DSM 1863 for L-malic acid production. *Fermentation* **8**(1):26 (2022).
27. Naude A and Nicol W, Fumaric acid fermentation with immobilised *Rhizopus oryzae*: quantifying time-dependent variations in catabolic flux. *Process Biochem* **56**:8–20 (2017). https://doi.org/10.1016/j.procbio.2017.02.027.
28. Krzystek L, Gluszcz P and Ledakowicz S, Determination of yield and maintenance coefficients in citric acid production by aspergillus Niger. *Chem Eng J Biochem Eng J* **62**(3):215–222 (1996). https://linkinghub.elsevier.com/retrieve/pii/0923046796030886.
29. Villadsen J, Nielsen J, Lidén G, Bioreaction Engineering Principles [Online]. 3rd ed. Media. Boston, MA: Springer (2011). Available: http://books.google.com/books?hl=en&lr=&id=htUeM34b7KgC&oi=fnd&pg=PR8&dq=Bioreaction+engineering+principles&ots=OYAiewkiRp&sig=_OrIEeYgQxEbBKI4QoCfFT-OEzQ [30 January 2012].
30. Zeitz MA, Tanveer Z, Openshaw AT and Schmidt M, Genetic regulators and physiological significance of glycogen storage in Candida albicans. *J Fungi* **5**(4):1–12 (2019).
31. Ruiz-Herrera J and Ortiz-Castellanos L, Cell wall glucans of fungi. A review. *Cell Surf* **5**(March):100022 (2019). https://doi.org/10.1016/j.tcsw.2019.100022.
32. Jeennor S, Anantayanon J, Panchanawaporn S, Khoomrung S, Chutrakul C and Laoteng K, Reengineering lipid biosynthetic pathways of *Aspergillus oryzae* for enhanced production of γ-linolenic acid and dihomo-γ-linolenic acid. *Gene* **706**(April):106–114 (2019). https://doi.org/10.1016/j.gene.2019.04.074.
33. Kaur P and Worgan JT, Lipid production by *Aspergillus oryzae* from starch substrates. *Eur J Appl Microbiol Biotechnol* **16**(2–3):126–130 (1982).
34. Jeennor S, Anantayanon J, Panchanawaporn S, Chutrakul C and Laoteng K, Morphologically engineered strain of *Aspergillus oryzae* as a cell chassis for production development of functional lipids. *Gene* **718**(August):144073 (2019). https://doi.org/10.1016/j.gene.2019.144073.
35. Muniraj IK, Xiao L, Hu Z, Zhan X and Shi J, Microbial lipid production from potato processing wastewater using oleaginous filamentous fungi *Aspergillus oryzae*. *Water Res* **47**(10):3477–3483 (2013). https://doi.org/10.1016/j.watres.2013.03.046.
36. Thammarongtham C, Nookaew I, Vorapreeda T, Srisuk T, Land ML, Jeennor S *et al*., Genome characterization of oleaginous *Aspergillus oryzae* BCC7051: a potential fungal-based platform for lipid production. *Curr Microbiol* **75**(1):57–70 (2018).
37. Anantayanon J, Jeennor S, Panchanawaporn S, Chutrakul C and Laoteng K, Significance of two intracellular triacylglycerol lipases of *Aspergillus oryzae* in lipid mobilization: a perspective in industrial implication for microbial lipid production. *Gene* **793**(May):145745 (2021).
38. Di Caprio F, A fattening factor to quantify the accumulation ability of microorganisms under N-starvation. *New Biotechnol* **66**(April):70–78 (2022). https://doi.org/10.1016/j.nbt.2021.04.001.
39. Athenaki M, Gardeli C, Diamantopoulou P, Tchakouteu SS, Sarris D, Philippoussis A *et al*., Lipids from yeasts and fungi: physiology, production and analytical considerations. *J Appl Microbiol* **124**(2):336–367 (2018).
40. Adeleke R, Nwangburuka C and Oboirien B, Origins, roles and fate of organic acids in soils: a review. *South African J Bot* **108**:393–406 (2017).
41. Ström L, Owen AG, Godbold DL and Jones DL, Organic acid behaviour in a calcareous soil implications for rhizosphere nutrient cycling. *Soil Biol Biochem* **37**(11):2046–2054 (2005). https://linkinghub.elsevier.com/retrieve/pii/S0038071705001367.
42. Pitt D and Ugalde UO, Calcium in fungi. *Plant Cell Environ* **7**(6):467–475 (1984 Aug). https://onlinelibrary.wiley.com/doi/10.1111/j.1365-3040.1984.tb01437.x.
43. Lange M and Peiter E, Calcium transport proteins in fungi: the phylogenetic diversity of their relevance for growth, virulence, and stress resistance. *Front Microbiol* **10**:3100 (Jaunary)(2020).
44. Ronoh DK, Swart RM, Nicol W and Brink H, The effect of pH, metal ions, and insoluble solids on the production of fumarate and malate by Rhizopus delemar in the presence of CaCO3. *Catalysts* **12**(3):263 (2022).

Hendrik G. Brink

Hendrik G. Brink completed his PhD in chemical engineering in 2015, specializing in bioreaction engineering. He was appointed in the Department of Chemical Engineering at the University of Pretoria in September 2015. During his tenure he has published 73 papers, has been cited 304 times, and currently has an H-index of 10. He has successfully supervised/co-supervised 14 master degree candidates and one PhD candidate, and currently supervises/co-supervises nine master degree and four PhD candidates. His research mainly focuses on waste valorization towards a circular economy.

Monique Geyer-Johnson

Monique Geyer-Johnson is currently working as a biologics manufacturing lead at Oxford Nanopore Technologies plc in the UK. She completed her master of engineering at the University of Pretoria in South Africa. As part of the chemical engineering department, she studied the malic acid producing capabilities of *Aspergillus oryzae* (aka Perry).

Reuben M. Swart

Reuben M. Swart recently completed his PhD in chemical engineering with research focused on biological fermentation. Specifically, he worked with a fungus (*Rhyzopus oryzae*) to produce value-added chemicals from sugars. He is now working as a post doc for the National Renewable Energy Laboratory on a microbial carbon capture project.

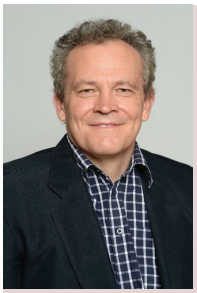

Willie Nicol

Willie Nicol leads the bioreaction engineering group at the University of Pretoria. The group's expertise is in real-time chemical manipulation of the envirome in contact with living organisms. The group's single culture work entails the production of fumaric, succinic, and malic acids from carbohydrates using bacterial and fungal strains. More recently, the focus shifted to the application of the envirome control concept to hydroponic and mixed culture bioreactors.